Shape selection through epitaxy of supported platinum nanocrystals

Laurent Peres, Deliang Yi, Susana Bustos-Rodriguez, Cécile Marcelot,
Alexandre Pierrot, Pier-Francesco Fazzini, Ileana Florea, Raul Arenal,
Lise-Marie Lacroix, Bénédicte Warot-Fonrose, et al.

HAL Id: hal-02001918

https://hal.insa-toulouse.fr/hal-02001918

Submitted on 21 Nov 2020

Journal Name

COMMUNICATION

Shape-selection through epitaxy of supported platinum nanocrystals

Laurent Peres,[a] Deliang Yi,[a] Susana Bustos-Rodriguez,[a] Cécile Marcelot,[b] Alexandre Pierrot,[a] Pier-Francesco Fazzini,[a] Ileana Florea,[c] Raul Arenal,[d,e] Lise-Marie Lacroix,[a] Bénédicte Warot-Fonrose,[b] Thomas Blon,[a] and Katerina Soulantica*[a]

Supported nanocrystals of original shapes are highly desirable for the development of optimized catalysts, however, conventional methods for the preparation of supported catalysts do not allow shape control. In this work we have synthesized concave platinum nanocubes exposing {110} crystallographic facets at 20°C. In the presence of a crystallographically oriented Pt(111) support in the reaction medium, the concave nanocubes grow epitaxially on the support, producing macroscopic nanostructured surfaces. Higher reaction temperature produces a mixture of different nanostructures in solution, however, only the nanostructures growing along the <111> direction are obtained on the Pt(111) support. Therefore, the oriented surface acts as a template for a selective immobilization of specific nanostructures out of a mixture, which can be regarded as an "epitaxial resolution" of an inhomogeneous mixture of nanocrystals. Thus, a judicious choice of the support crystallographic orientation may allow isolating original nanostructures, that cannot be obtained in a pure form.

The intensive research on metal nanocrystal synthesis is associated to a significant degree to the optimization of their catalytic properties. The performances of catalysts being dependent on nanocrystal structural characteristics such as type and number of exposed facets, tailoring of metal nanocrystals morphology is an active area of ongoing research.[1-3] Wet-chemistry methods of nanoparticle synthesis open new perspectives in the domain of well-controlled and thus sustainable catalysts since they are the best adapted for the large-scale preparation of size-, shape- and composition-controlled metal nanocrystals.[4-6] However, in many cases original nanostructures are formed in solution not as the unique product, but together with different nano-objects. Unsupported nanocrystals used as catalysts have limited stability and they cannot be easily isolated/recycled. On the other hand, conventional methods for the preparation of supported catalysts allow little control over nanoparticle shape.[7] The possibility to immobilize shape-controlled nanostructures exposing specific surfaces on supports offers the opportunity (i) to increase their stability towards aggregation/sintering as compared to their non-supported counterparts, (ii) to explore them as model catalysts in configurations that better approach the complexity of real catalytic systems than the single crystal model catalysts,[8] and (iii) provided that stabilizing ligands can be eliminated or exchanged, to establish structure-performance relationships or study ligand effects respectively. We have previously shown that a wet-chemistry method that produces well-defined and homogeneously shaped nano-objects in solution can reproduce these nano-objects on a solid support by performing the reaction in the presence of this support. By this method it has been possible to epitaxially grow cobalt nanowires and iron nanocubes on crystallographically oriented metal surfaces,[9,10] as well as on bulk metal foams.[11] It was also shown that the epitaxial relationship between the support and the growing nanostructure determines the orientation of the nanostructure on the support surface, while the composition of the solution determines the nanostructure shape, which corresponds to the same shape obtained in solution in the absence of support, thus, to the same exposed facets.[10] Platinum is one of the most active metals for a large spectrum of catalytic reactions. Here we report the growth of pure Pt concave nanocubes, exposing {110} facets, both in solution and on Pt(111) crystallographically oriented metal supports, by using a simple and low-cost precursor (PtCl$_2$) at an unprecedently low temperature. To our

a. *Laboratoire de Physique et Chimie des NanoObjets (LPCNO), Université de Toulouse, CNRS, INSA, UPS, 135 avenue de Rangueil, 31077 Toulouse, France..*
b. *Centre d'Elaboration de Matériaux et d'Etudes Structurales (CEMES-CNRS), 29 rue Jeanne Marvig, B.P. 94347, 31055 Toulouse, France.*
c. *Laboratoire de Physique des Interfaces et des Couches Minces (LPICM), Ecole Polytechnique/CNRS, Route de Saclay, 91128 Palaiseau Cedex, France.*
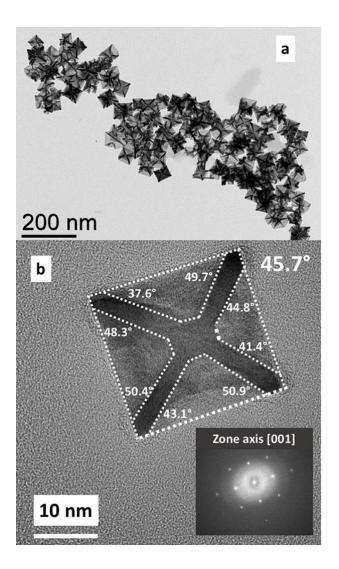d. *Instituto de Nanociencia de Aragon (INA), Universidad de Zaragoza, Calle Mariano Esquillor, 50018 Zaragoza, Spain..*
e. *ARAID, 50018 Zaragoza, Spain.*

† Footnotes relating to the title and/or authors should appear here.
Electronic Supplementary Information (ESI) available: [details of any supplementary information available should be included here]. See DOI: 10.1039/x0xx00000x

knowledge, pure Pt nanocrystals exposing {110} facets have not been reported in the literature, and the low temperature is a key parameter for their formation. More importantly, while higher temperature leads to various growth modes of the nano-objects in solution, only one type of growth direction is allowed on the surface of the Pt(111) support. This corresponds to a selection by the support of only the matching nano-objects among the different possibilities. Therefore, even when morphological homogeneity is not achieved by a wet-chemistry approach, the introduction during synthesis of a crystallographically oriented support in the reaction medium can induce the growth on the support of only the epitaxially compatible nanostructure among the ones formed in solution.

Briefly, the metal precursor and an excess of octadecylamine (ODA) were mixed in toluene and then let to react under H_2 (see ESI† for experimental details). Fig. 1 displays Transmission Electron Microscopy (TEM) and High Resolution TEM (HRTEM) micrographs of the nano-objects obtained after one-week reaction at 20°C. The long reaction time is necessary for total Pt transformation at this very low reaction temperature.

Fig. 1 (a) low magnification TEM micrograph of concave Pt nanocubes obtained at 20°C (1-week reaction). (b) HRTEM of an individual Pt nanocube with the measured dihedral angles, showing a mean angle of 46°; in inset the corresponding Fast Fourier Transform (FFT) of of the Pt nanocube oriented along the [001] zone axis.

Among various conventional and nonconventional shape-controlled nanoparticles, concave nanocrystals of noble metals crystallized in the face-centered cubic (fcc) structure present a specific interest for catalysis because they are enclosed by higher energy facets, thus more active, than the thermodynamically favored and usually exposed {111} and {100} low index ones.[12-14] To determine the nature of the facets exposed by the concave nanocubes obtained, we have measured the angle formed between the projection of a given facet and the (100) crystallographic planes that would enclose an ideal cube. The measurement has been performed on a total number of 55 nanocubes giving a mean value of ca. 46° (Fig. 1b), which corresponds to {110} facets (theoretical value 45°).[15] Furthermore, in order to get precise and direct information about the 3D morphology and structure of these Pt nanocubes, we have performed Electron Tomography (ET) studies in the Scanning TEM(STEM)–High-Angular Annular Dark Field (HAADF) imaging mode.[16,17] Fig. S1 ESI† presents a schematic representation of orthogonal slices taken at two different orientations through the reconstructed volume that unambiguously evidence the presence of (100), (010) and (001) crystallographic planes. The nanocubes mean size is 45.1 ± 7.7 nm. The XRD diffractogram is presented in Fig. S2 ESI† and shows the peaks corresponding to fcc Pt.

Platinum-based nanoparticles among which concave nanocrystals, especially nanocubes, have been prepared by several groups and are actively studied mainly as electrocatalysts,[15,18-22] but also in thermal catalysis.[23,24] While many concave nanocrystals exposing different (hkl) facets corresponding to different degrees of concavity have been reported, concave nanocubes of pure Pt exposing {110} facets have not been reported so far, despite the fact that bimetallic Pt-containing concave nanocubes enclosed by {110} facets already exist.[15] While platinum nanocrystals of controlled shape exposing exclusively {100} or {111} and a mixture of these two facets have been used in order to study structure-performance relationships in heterogeneous catalytic reactions,[25-27] Pt nanoparticles exposing {110} facets being unavailable, no such studies were possible for these facets. Pt {110} surfaces prepared by ultra-high vacuum techniques have been studied as model catalysts.[28] The {110} facets expose second layer atoms, thus, despite the fact that they are low index facets, they are composed of a high number of atoms of low coordination number, and as such they are expected to be highly active.[12]

We have monitored the growth process by stopping the reaction at different time intervals. Surprisingly, even after one hour of reaction, we can notice already the formation of

concave nanocubes, along with ill-shaped nano-objects, and small classical cubes. While a formation mechanism at the molecular level is not possible to establish from the data available, it is likely that these small cubes constitute the seeds on which adsorption of Pt adatoms on the corners and their subsequent surface diffusion only along the edges allows obtaining the concave cubes.[29] Increasing the reaction time results in a better definition of the shape and improvement of the size distribution (Fig. S3, ESI†). This could be due to a ripening process induced by Cl$^-$. A Pt atom exchange between solid and solution phases, could also account for a surface reconstruction of the initially formed ill-shaped nanocrystals, eliminating them in favour of more regular shapes from which the growth of the concave cubes can continue. Reducing the temperature to 15°C for the same reaction time (7 days) yields concave cubes of small size and a large size distribution. Other less well-defined shapes can also be observed. A small increase of the temperature from 20 to 30°C slightly affects the nanocubes concavity which seems to be less pronounced compared to the concave cubes obtained at 20°C. The, the low reaction temperature is necessary for the formation of the metastable concave nanocubes exposing {110} facets. The key for obtaining this specific morphology is a fine equilibrium between the rate of Pt atom deposition on the vertices and the one of its diffusion on the edges of the initially formed seeds. For this to happen, several conditions have to be fulfilled, among which the use of the long chain amine, which plays a double role, as a modulator of the $PtCl_2$ reactivity towards H_2 and as a capping agent. ODA reacts with $PtCl_2$ to give complexes which can be reduced by H_2 at room temperature, and it does so at a rate that allows diffusion along the edges, a prerequisite for the formation of the cubs enclosed by {110} facets. Therefore, the first role of ODA is to regulate the reduction rate and by this the rate of Pt atom supply. In this context, the choice of the precursor is also pivotal for obtaining the concave morphology because through reaction with ODA it allows the formation of species that can supply Pt units at an appropriate rate. The role of the amine as a coordinator of the kinetics is not universal but precursor dependent. Replacing $PtCl_2$ by H_2PtCl_6, while keeping the rest of the reaction parameters identical to the ones that yield concave nanocubes, does not produce nanoparticles at 20°C due to the higher stability of Pt(VI) towards reduction. TEM observations show that the nano-objects formed at shorter reaction times are embedded in a matrix, which we attribute to Pt containing species that constitute the reservoir. This material, which can be discerned even after 48h reaction (Fig. S3, ESI†), is diminishing as reaction goes to the end. Indeed, the Pt yield is about 60% after 48h of reaction and 90% after one-week reaction. The oxidation state of the Pt reservoir is not known, and we cannot exclude a complete reduction at short reaction times, the fact that at 48h (Fig. S3, ESI†) we have a bimodal size distribution points toward a low supersaturation of the solution in Pt atoms, which results in nucleation and growth taking place at comparable rates. Apart from being a regulator of the reduction kinetics, ODA can also passivate the Pt

facets. Further studies are in progress in order to better understand the particular effect of the different species on the growth of the**se** nanostructures, but probably ODA stabilizes preferentially the less compact {110} facets.

At 60°C, 24h reaction time is sufficient to reduce the entire Pt and the main product is octopods, some presenting outgrowths on their branches, while scarce less symmetrical objects with long branches start to appear. We assume that increasing the temperature favours a faster Pt atom deposition on the vertices, which does not let enough time for diffusion towards the edges to occur.[29] At 80°C and 24 h reaction, the dendritic octopods are still dominant, while the objects with long branches are less scarce (Fig. S4, ESI†). However, at 100°C, for a reaction time of 24h, the formation of a majority of multipods is observed along with less abundant dendritic octopods (Fig. 2). The XRD diffractogram of the 100°C product is presented in Fig. S5 ESI†.
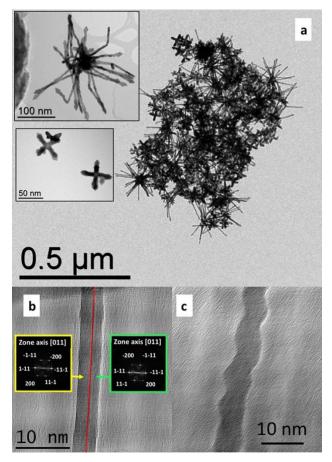

Fig. 2 (a) TEM image of the nano-objects obtained at 100° C (24 h of reaction). In the insets magnifications of the two types of objects obtained: multipods and octopods with outgrown domains on the branches. (b), (c) two HRTEM images corresponding to two different orientations of the multipods branches. The red line in (b) corresponds to a twin (111) type plane.

Obviously, the octopods result from a growth along the <111> directions of cubic seeds. They are similar to the dendritic

nanocubes obtained previously by some of us and proposed to be enclosed mainly by (100) type planes.[30] However, HRTEM analysis of the multipodes has shown that there is not a common growth direction between the branches of the multipodes and the ones of the octopods. In Fig. 2b and c we present the HRTEM images of two multipod branches oriented differently with respect to the electron beam. Whereas the cores of the multipods are not clearly distinguished, HRTEM observation of the multipod branches shows a twin boundary that can be discerned when the arms are observed along the [001] zone axis (Fig.2b). These arms grow along a <112> type direction and the twin plane corresponds to a (111) type plane. Thus, the enclosing smooth facets parallel to this plane are of the {111} type. While observation along this zone axis shows a smooth contour, their three-dimensional shape can be understood by observing the TEM images of several of these arms which present a saw-like contour (schematic representation in Fig. S6 ESI†). Resembling twinned branches on three-fold symmetry Pt nano-objects have been previously observed by others[31, 32] and by some of us,[33] and the facets exposed by those nano-objects had been proposed as being mostly {111} with a small fraction of {100} facets. The reaction at 100°C was stopped at 5 min, 20 min, and 1h in order to follow the evolution of the nanocrystals at early growth stages by TEM. As can be observed in Fig. S7 ESI† at 5 min we can notice the presence of nanocrystals of cubic symmetry (cubes, concave cubes), nanostructures of three-fold symmetry, as well as objects with lower symmetry. At 20 min nanoobjects of disparate shapes and sizes are present. We start to distinguish octopods and multipods, as well as newly formed nanocrystals. At 1h the growth of the multipod branches is more pronounced and the octopods have started to develop outgrowths on their branches. Branches containing (111) twin planes and growing along <112> type direction can stem out of three-fold symmetry twinned seeds, or from multiply twinned seeds giving rise to tripods and multipods respectively[31, 32] via a "twin-trough" growth model. We believe that upon increasing the temperature we favour the formation of twinned seeds from which growth along <112> directions ends up in forming the saw-like branches. It is possible that coalescence or oriented attachment between twinned seeds forms a more complex core, from which a large number of branches can grow.

We have applied the method of solution epitaxial growth of nanocrystals on crystallographically oriented thin films by simply introducing in the reaction mixture a Pt(111) thin film epitaxially grown by sputtering deposition on a α-Al_2O_3(0001) substrate (see ESI† and refs. 9, 10). We have thus grown Pt nanostructures on Pt(111) surfaces at 25°C and 100°C. While the reaction at 25°C presented the opportunity of elaborating supported nanoparticles presenting {110} facets, the reaction at 100°C was especially well-adapted in order to find out whether an epitaxial growth mode could favour the development of nano-objects that grow only along the <111> direction, that is, branches of octopods, even if in the absence of support the same reaction produces a mixture of nanocrystals in which the branched octopods are less abundant. The results of the reaction at low temperature are shown in Fig.3. After 7 days at 25°C, we observe the presence of concave nanocubes exposing {110} facets in the supernatant solution, due to the simultaneous homogeneous nucleation (Fig. S8 ESI†). Scanning Electron Microscopy (SEM) images of the support are shown in Fig. 3a. The increase from 20°C to 25°C of the reaction temperature did not impact the nanostructure shape, while at the same time it allowed a higher density of nanostructures to be grown on the substrate, thus an easier observation of the cross-section. A dense heterogeneous nucleation on the support has given rise to a growth of nano-structures of an apparent three-fold symmetry. These are concave nanocubes which have grown epitaxially on the Pt(111) film, thus with their (111) planes parallel to the (111) planes of the support. For facilitating visualisation of the growth mode, we show in Fig 3b a schematic representation of nanocubes grown on the support and in Fig. 3c a single nanocube on the support as it appears when viewed from the top. The epitaxial growth results in a common in-plane orientation of the majority of the cubes. It has to be noted that a rotation by 60° results in the same epitaxy. A definitive proof of the homoepitaxial relationship is given by observation of a cross-section of the sample (Fig. 3d, e) with identical FFT patterns performed on nanocube and film respective areas of the HRTEM cross-sectional micrograph (Fig. 3e). In agreement with the analysis by microscopy, XRD measurements are consistent with an epitaxial growth since no other reflections than the Pt(111) are observable (Fig. S9a ESI†).
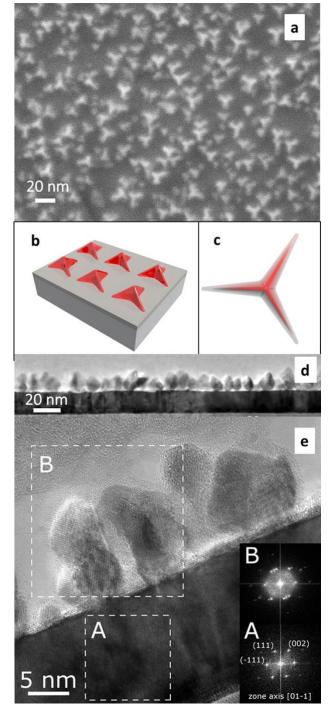
COMMUNICATION

Fig. 3 (a) SEM of the support after nanocube growth (7 days, 25°C). (b) schematic representation of the concave nanocubes grown on the support. (c) one nanocube observed from the top. (d) TEM and (e) HRTEM images the of cross-section evidencing the epitaxial growth of the concave nanocubes on Pt(111) (inset: FFT patterns obtained on the Pt film (A) and nanocubes respective areas (B)).

Increasing the temperature to 100°C in the presence of the Pt(111) support yields a dense array of oriented and organized Pt elongated and branched nanostructures (Fig. 4). Examination by TEM of the supernatant shows that homogeneous nucleation has resulted in the formation of multipods and dendritic octopods in solution (Fig. S10 ESI†) as described above (Fig. 2). TEM cross-sectional views (Fig 4b) of the support after reaction show the presence of dendritic branches of Pt grown on the

Pt(111) film, constituting a quite homogeneous layer of about 50 nm thickness. The HRTEM observation of the sample obtained at 100°C (Fig. 4c), as in the case of the concave nanocubes (Fig. 3e), demonstrates the continuity between the (111) planes of the thin film and the NPs grown, and also the common [011] zone axis, confirming the homoepitaxial relationship Pt(111)[011] // Pt(111) [011] between NPs and the film.
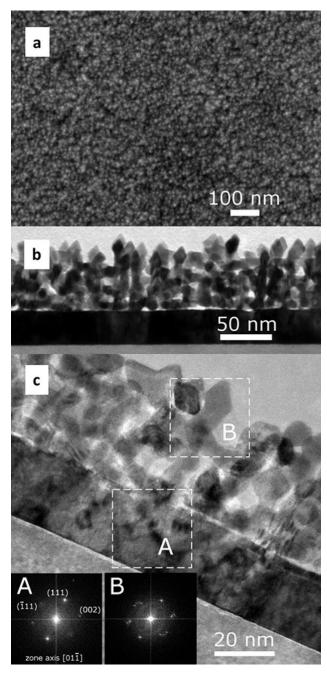

Fig. 4 (a) SEM of the support after Pt dendritic arms growth. (b) TEM of a cross-section of the support. (c) HRTEM images the cross-section evidencing the epitaxial growth of the nanostructures (inset: FFT patterns obtained on the Pt film (A) and on branches respective areas (B)).

The XRD of the Pt(111) support after the growth of the Pt nanostructures at 100°C presents the Pt(111) reflections

exclusively (Fig. S9b ESI)†. Interestingly, this means that among the possible nanostructures that can be formed under these experimental conditions in solution, the support "selects" only the ones that grow along the <111> direction. This selectivity could be regarded as a resolution through epitaxy of a mixture of nanostructures. Thus, homogeneously shaped nano-objects can be developed by epitaxial growth on crystallographically oriented surfaces, even if the solution from which they grow can produce a mixture of different nano-structures. Apart from the general fundamental interest that this concept presents, it can offer the possibility to immobilize original nanostructures that are produced together with other nanocrystals by wet-chemistry, but are not accessible in a pure form. The establishment of structure-performance relationships is an important challenge in heterogeneous catalysis and it depends on the possibility to synthesize well-defined catalytic nanoparticles.[34] Surface science studies of defect-free, single-crystal model catalysts play a pivotal role in underpinning structure-activity relationships and elementary reaction mechanisms in catalytic reactions.[35-37] However, these model catalysts do not present various important features characteristic of real heterogeneous catalysts. In a perspective, the as-obtained supported nanostructures could reduce the materials gap as model catalysts, providing a range of features (edges and corners) present in real catalysts but absent from single crystal model catalysts.[8] Indeed, the nanostructured supports obtained at 25°C are especially interesting because they bear epitaxially grown nano-objects exposing {110} facets, which were not available up to now. It has to be noted that ligands are still present on the surface after washing. While ligands can be beneficial to several catalytic reactions,[38-40] structure-performance relationships concerning specific facets would require ligand removal, which should be possible without any coalescence thanks to the robust Pt-Pt interface between the support and the nanostructures which should also prevent easy sintering.

Conclusions

In conclusion, we have synthesized at room temperature the first pure-Pt concave nanocubes exposing {110} facets, using $PtCl_2$ as a precursor in the presence of ODA. The key for obtaining the Pt concave nanocubes exposing {110} facets is a coordination between Pt atom deposition and its diffusion. The combination of $PtCl_2$ as a precursor and of the long chain amine, which plays a double role, as a modulator of the $PtCl_2$ reactivity towards H_2 and as a capping agent, are crucial. Increasing the reaction temperature to 100°C gives rise to a mixture of dendritic octopods and multipods. If a crystallographically oriented Pt(111) thin film is introduced in the solution during the reactions, epitaxially grown concave nanocubes and nanodendrites are obtained at low and high temperature respectively. Interestingly, the results at 100°C show that a crystallographically oriented support, present in a reaction mixture giving rise to a variety of nano-objects of different shapes, can select the type of nano-objects growing on its surface, according to their growth direction. Having the possibility to selectively immobilize on a surface only

nanostructures growing along a certain growth direction among several co-existing nanostructures in the reaction medium, could also allow obtaining the most desired nanostructure by a judicious choice of the crystallographically oriented surface that will be introduced in the reaction medium. Such an approach opens the perspective of introducing supports of different crystallographic orientations in the same solution and reproduce only one type of nanostructre on each support. Apart from its general importance, such a process of recognition and selective growth of supported nanostructures is of special interest in the engineering of model catalysts.

Conflicts of interest

There are no conflicts to declare.

Acknowledgments

Notes and references

1 J. Pal and T. Pal, *Nanoscale*, 2015, **7**, 14159-14190.
2 F. Zaera, *Chem. Soc. Rev*., 2013, **42**, 2746-2762.
3 N. Sharma, H. Ojha, A. Bharadwaj, D. P. Pathak and R. K. Sharma, *RSC Adv*., 2015, **5**, 53381- 53403.
4 J. Watt, S. Cheong, R. D. Tilley, *Nano Today*, 2013, **8**, 198-215.
5 G. J. Leonga, M. C. Schulzea, M. B. Stranda, D. Maloneya, S. L. Friscoa, H. N. Dinhb, B. Pivovarb and R. M. Richards, *Appl. Organometal. Chem*., 2014, **28**, 1–17.
6 Z. Fan and H. Zhang, *Chem. Soc. Rev*., 2016, **45**, 63-82.
7 P. Munnik, P.E. de Jongh and K. P. de Jong, *Chem.Rev*., 2015, **115**, 6687-6718.
8 H. A. Doan, M. K. Sharma, W. S. Epling, and L. C. Grabow, *ChemCatChem* 2017, **9**, 1594-1600.
9 N. Liakakos, T. Blon, C. Achkar, V.Vilar, B. Cormary, R. P.Tan, O. Benamara, G. Chaboussant, F. Ott, B. Warot-Fonrose, E. Snoeck, B.Chaudret, K. Soulantica and M. Respaud, *Nano Lett*., 2014, **14**, 3481–3486.
10 N. Liakakos, C. Achkar, B. Cormary, J. Harmel, B.Warot-Fonrose, E. Snoeck, B. Chaudret, M. Respaud, K. Soulantica and T. Blon, *ACS Nano*, 2015, **9**, 9665–9677.
11 J. Harmel, L. Peres, M. Estrader, A. Berliet, S. Maury, A. Fécant, B. Chaudret, P. Serp and K. Soulantica, *Angew. Chem. Int. Ed*., 2018, **57**, 10579-10583.
12 J. Zhang, Q. Kuang, Y. Jiang and Z. Xie, *NanoToday*, 2016, **11**, 661-677.

13 Q. Chen, Y. Jia, S. Xie, and Z. Xie, *Chem. Soc. Rev*. 2016, **45**, 3207–3220.

14 H. Zhang, M. Jin, and Y. Xia, *Angew. Chem. Int. Ed*., 2012, **51**, 7656–7673.

15 Q. Chen, Y. Yang, Z. Cao, Q. Kuang, G. Du, Y. Jiang, Z. Xie and L. Zheng. *Angew. Chem. Int. Ed*., 2016, **55**, 9021 –9025.

16 I. Florea, C. Feral-Martin, J. Majimel, D. Ihiawakrim, C. Hirlimann and O. Ersen, *Cryst. Growth Des*. 2013, **13**, 1110–1121.

17 F. L. Deepak, A. Mayoral, R. Arenal, in Advanced Transmission Electron Microscopy: Applications to Nanomaterial; Eds.; Springer International Publishing: Cham, Switzerland, 2015.

18 B.-A. Lu, J.-H. Du, T. Sheng, N. Tian, J. Xiao, L. Liu, B.-B. Xu, Z.-Y. Zhou and S.-G. Sun. *Nanoscale,* 2016, **8**, 11559–11564.

19 T. Yu, D. Y. Kim, H. Zhang, and Y. Xia, *Angew. Chem. Int. Ed*., 2011, **50**, 2773–2777.

20 B. Y. Xia, H. B. Wu and X. W. Lou, *Angew. Chem. Int. Ed.,* 2013, **52**, 12337–12340.

21 X. Xu, X. Zhang, H. Sun, Y. Yang, X. Dai, J. Gao, X. Li, P. Zhang, H.-H. Wang, N. F. Y and S.-G. Sun*, Angew. Chem. - Int. Ed*. 2014, **53**, 12522–12527.

22 Y. Lu, Y. Jiang, and W. Chen, *Nanoscale*, 2014, **6**, 3309–3315.

23 C. Wang, C. Lin, L. Zhang, Z. Quan, K. Sun, B. Zhao, F. Wang, N. Porter, Y. Wang and J. Fang, *Chem. Eur. J.,* 2014, **20**, 1753–1759.

24 Y. Gu, Y. Zhao, P. Wu, B. Yang, N. Yang and Y. Shu, *Nanoscale*, 2016, **8**, 10896–10901.

25 T.S. Ahmadi, Z.L. Wang, T.C. Green, A. Henglein and M.A. El-Sayed, *Science*, 1996, **272**, 1924- 1926.

26 K.M. Bratlie, H. Lee, K. Komvopoulos, P. Yang and G. A. Somorjai, *Nano Lett*., 2007, **7**, 3097-3101.

27 I. Lee, R.Morales, M. A. Albiter and F. Zaera, *Proc. Natl. Acad. Sci.*, 2008, **105**, 15241–15246.

28 B. L. M. Hendriksen and J. W. M. Frenken, *Phys. Rev. Lett*., 2002, **89**, 046101.

29 X. Xia, S. Xie, M.Liu, H.-C. Peng, N.Lu, J. Wang, M. J. Kim, and Y. Xia. *Proc. Natl. Acad. Sci.,* 2013, **110**, 6669–6673.

30 L.-M. Lacroix, C. Gatel, R. Arenal, C. Garcia, S. Lachaize, T. Blon, B. Warot-Fonrose, E. Snoeck, B. Chaudret and G. Viau, *Angew. Chem. Int. Ed*. 2012, **51**, 4690 –4694.

31 S. Maksimuk, X. Teng and H. Yang, *J. Phys. Chem. C*, 2007, 111, 14312-14319.

32 M.Tsuji, P. Jiang, S.Hikino, S. Lim, R. Yano, S.-M. Jang, S.-H. Yoon, N.Ishigami, X. Tang, K.S.N. Kamarudin, *Colloids Surf. A*, 2008, **317**, 23-31.

33 B. Cury Camargo, B. Lassagne, R. Arenal, C. Gatel, T. Blon, G. Viau, L.-M. Lacroix and W. Escoffier, *Nanoscale*, 2017**, 9**, 14635-14640.

34 L. Liu and A. Corma, *Chem. Rev*., 2018, **118**, 4981-5079.

35 U. Hejral, P. Müller, O. Balmes, D. Pontoni and A. Stierle, *Nat. Commun*. 2016, **7**, 10964.

36 vJ. Dou, Z. Sun, A. A. Opalade, N. Wang W. Fu and F. Tao, *Chem. Soc. Rev*., 2017, **46**, 2001-2027.

37 K. Cao, J. Cai, X. Liu and R. J. Chen, *Vac. Sci. Technol. A*, 2018, **36**, 010801.

38 S. Campisi, M. Schiavoni, C. Chan-Thaw and A. Villa, *Catalysts*, 2016, **6,** 185.

39 L. Jin, B. Liu, S. Duay and J. He, *Catalysts*, 2017, **7**, 44.

40 W. Huang, Q. Hua and T. Cao, *Catal. Lett*., 2014, **144**, 1355–1369.